COOLANT PASSAGE HEAT TRANSFER WITH ROTATION*

T. J. Hajek
United Technologies Corporation
Pratt and Whitney

J. Wagner and B. V. Johnson
United Technologies Research Center

In current and advanced gas turbine engines, increased speeds, pressures and temperatures are used to reduce specific fuel consumption and increase thrust/weight ratios. Hence, the turbine airfoils are subjected to increased heat loads escalating the cooling requirements to satisfy life goals. The efficient use of cooling air requires that the details of local geometry and flow conditions be adequately modeled to predict local heat loads and the corresponding heat transfer coefficients.

Improved turbine airfoil local temperature and hence, life predictions can be realized by accurately accounting for the effects of rotation on internal cooling. Although the effects of rotation which give rise to Coriolis and buoyancy forces can be large, they are currently not adequately included in the heat transfer designs of blades. Experimental data is particularly needed for the higher Rayleigh and Reynolds number conditions that are characteristic of turbine airfoils cooling passages. This data is crucial for development of design correlations and computer codes as well as their verification. Accurate prediction of local heat transfer coefficients enables the designer to optimize cooling configurations to minimize both metal temperature levels and thermal gradients. Consequently, blade life and engine efficiency can be significantly improved.

OBJECTIVE

The objective of this 36-month experimental and analytical program is to develop a heat transfer and pressure drop data base, computational fluid dynamic techniques and correlations for multi-pass rotating coolant passages with and without flow turbulators. The experimental effort is focused on the simulation of configurations and conditions expected in the blades of advanced aircraft high pressure turbines. With the use of this data base, the effects of Coriolis and buoyancy forces on the coolant side flow can be included in the design of turbine blades.

EXPERIMENTAL MODEL

The coolant passage heat transfer model features a four-pass serpentine arrangement designed to reflect the passages within a gas turbine blade. For the present experiments, the model was fitted with skewed turbulators, as indicated in figure 1. Figure 2 shows a schematic diagram of the model with the instrumentation and wall sections indicated. Heat transfer coefficients are obtained for each wall section element. These wall elements, numbered 1 to 64, consist of a copper block backed with a thin film electrical resistance type heater and instrumented with two thermocouples. The copper wall sections are 10.7 mm x 49.3 mm (0.42 in. x 1.94 in.). Each section is thermally isolated from the adjoining section by a 1.5 mm (0.060 in.) thick divider strip of low thermal conductivity G-11 composite material. The straight radial passages have a square cross section, 12.7 mm x 12.7 mm (0.5 in. x 0.5 in.).

*NASA Contract NASA-23691

DATA REDUCTION

Data acquisition/analysis consists of three general categories: equipment calibration, model heat loss measurement, and heat transfer coefficient calculations. The equipment calibration follows standard experimental procedures. Model heat loss measurements precede each test. These measurements are executed with no coolant flow and uniform wall temperature steady-state conditions, identical to the subsequent test less the coolant flow. Heat transfer coefficients are then calculated for each wall section element by applying the following procedure.

For each copper element the net energy convected to the fluid is calculated by subtracting the electrical line losses and conducted heat losses from the total energy supplied. Bulk fluid temperatures are then calculated based on an energy balance for each flowpath section as follows:

$$T_{b_{out}} = \frac{q_{net,\ 4\ walls}}{mc_p} + T_{b_{in}}$$

where the model inlet bulk temperature is measured. Once bulk fluid temperatures are determined, heat transfer coefficients are calculated from the equation:

$$h = \frac{q_{net,\ wall}}{A\ (T_w - T_b)}$$

where T_b is the average of the inlet and exit bulk temperatures. Thus for each test case, 64 heat transfer coefficients are calculated.

Table I shows the test conditions for which data were acquired with the skewed rough wall model. A total of 30 tests has been conducted to isolate the effects on heat transfer of rotation rate, flow rate, coolant-to-wall temperature variations, radius length and passage angle.

RESULTS

All of the experiments listed in Table I were completed to date. Measurements of both the passage heat transfer and the channel pressure drop were conducted. Due to the large number of data points obtained, comprehensive discussion of all the results is beyond the scope of this paper. Instead, the following paragraphs will mainly focus on comparisons between the smooth and the skewed trip strip channel data at specific operating conditions and physical locations within the model. This will facilitate better understanding of the underlying physical principles. It should also be noted that due to the complexity of the subject matter, many of the explanations presented herein are hypotheses and will require further substantiation.

In order to fully understand the channel heat transfer behavior under the influence of rotation, it is imperative that key differences between the smooth and the augmented channel be examined in stationary frame first. Figure 3 depicts a comparison between the smooth and augmented models for the baseline condition of Re = 25,000. In the first leg of the model, the smooth channel heat transfer exhibits classical thermal development behavior (decreasing Nusselt number with

distance), whereas the rough wall shows nearly constant augmentation (factor of 3) throughout the first leg. This is consistent with other Pratt & Whitney data.

Also quite different is the turn heat transfer. For the smooth wall case, classical heat transfer increase (factor of 2) is present. In the augmented channel turn, the Nusselt number decreases through the turns (note that it reaches values below the smooth duct). This is followed by an immediate increase, just downstream of the turn. Subsequently, the second leg heat transfer decreases along the passage. A similar pattern repeats for the second turn and the third leg. It is important to note that the second and the third passages exhibit progressively decreasing average Nusselt number. In fact, the third passage augmentation approaches levels expected from normal trip strips. Even though good understanding of this phenomenon has not been gained to date, it is clear that the first passage (with its well behaved inlet) acts very much like a straight duct, whereas the subsequent passages are strongly affected by the turn generated secondary flows. It is felt that this fact will play an important role in understanding the rotating results. Consistent with other results, the rough channel side wall (rib wall) heat transfer is augmented somewhat by the presence of the trip strips, but in general behaves similarly to the smooth duct rib walls.

Figure 4 shows comparison of heat transfer results for smooth wall and skewed trip rough wall at baseline rotating flow conditions of Ro = 0.24 and Re = 25,000. As was the case with the smooth passage, the rough wall leading surface heat transfer is significantly reduced (40-50% reduction) by the introduction of rotation. Because the trailing side shows heat transfer augmentation of only 30%, the average channel Nusselt number is reduced. While the rough model heat transfer in the first passage is strongly affected by rotation, the subsequent legs and turns show very little dependence. This fact is further supported by examining figure 5, where heat transfer ratios are presented for several rotation rates. In this figure, the first passage is again quite active, whereas the other channels exhibit very little variation with rotation. This finding further supports the hypothesis of turn generated secondary flows dominating the subsequent passages.

The influence of buoyancy on rotating channel heat transfer is depicted in figure 6. With the exception of the first leg, the leading (stabilized) wall shows very weak dependence on temperature (density) variations. The trailing surface, on the other hand, does show considerable dependence on ΔT. Better representation can be found in figure 7. Leading and trailing surfaces are plotted for the last heating element in the first leg. Note that the data at Ro = 0.0 do not coincide. This is a direct result of small manufacturing inconsistencies in the heating elements. The density (temperature) ratio is shown with flag symbols. It can be clearly seen that the trailing surface heat transfer is more sensitive to density variations than the leading surface. When the trailing side data are examined closely, it can be seen that the absolute heat transfer change due to temperature variations is approximately the same for both smooth and rough ducts. The rough wall leading surface, however, shows significantly smaller variation for a given ΔT change. This information indicates that the buoyancy forces do not play as important a role in augmenting heat transfer on "stabilized" surfaces for rough walls as they do for smooth walls. This fact is further supported in figure 8, where the same data is plotted against the Buoyancy Parameter. Both leading and trailing surfaces for smooth ducts as well as trailing surface for rough ducts correlate well with the Buoyancy Parameter. However, the leading surface data for the rough wall model do not collapse. Potentially, this may indicate that in addition to the buoyancy forces, some other process, as yet unexplained, is becoming important.

It should also be noted in figure 8 that at high levels of the Buoyancy Parameter, the heat transfer ratios are approaching an asymptotic limit. In the case of the smooth duct trailing surface, the limiting rough wall heat transfer level is only 20% higher.

In reality, the difference is only 10% if the rough wall convection area is corrected for the trip strip surface area. The important observation to be made here is that at low values of the Buoyancy Parameter, the rough wall has significant heat transfer advantage over the smooth wall. At high values of the buoyancy parameter, however, the trip strip advantage is significantly diminished.

WORK PLANNED

Detailed analysis and correlation of the skewed turbulator data will continue.

Currently the model is being modified to include normal turbulators on the leading and the trailing surfaces of the straight radial passages. A thirty point test matrix, similar to the one in Table I will be executed.

TABLE 1

TEST MATRIX FOR ROTATING HEAT TRANSFER EXPERIMENTS FOR SKEWED TURBULATORS

Test No.	UTRC Run No.	Dimensional Parameters						Basic Dimensionless Parameters					Secondary Dimensionless Parameters		
		P (psi)	Ω (rpm)	$\dot{m}$ (lb/sec)	ΔT (F)	H (in)	α (deg)	Re	Ro	$\frac{\Delta T}{T_{in}}$	$\frac{H}{d}$	$\frac{\Delta\rho}{\rho}\frac{\Omega H}{V}$	Gr/Re^2	$Grx10^{-8}$	Comments
201	6.7	147.7	0	0.013	81	25	0	25,337	0	0.15			0	0	No Rotation
202	9.9	147.8	0	0.006	80	25	0	12,490	0	0.15			0	0	
203	8.8	149.5	0	0.025	80	25	0	50,715	0	0.15			0	0	
204	10.8	145.0	0	0.024	80	25	0	75,348	0	0.15			0	0	
205			15		80	25	0	25,000	0.006				0.00	0.00	
206			145		80	25	0	25,000	0.06				0.01	0.13	
207			275		80	25	0	25,000	0.12				0.05	0.46	Vary Ro
208			412		80	25	0	25,000	0.18				0.12	1.06	Hold ΔT, Re
209			550		80	25	0	25,000	0.24				0.22	1.96	
210			825		80	25	0	25,000	0.35				0.45	4.22	
211			145		80	25	0	12,500	0.12				0.09	0.14	Vary Re
212			550		80	25	0	50,000	0.12				0.06	1.98	Hold ΔT, Ro
213			825		80	25	0	75,000	0.12				0.05	4.20	
214			275		160	25	0	25,000	0.12				0.14	0.87	High ΔT
215			550		160	25	0	50,000	0.12				0.14	3.49	
216			145		160	25	0	25,000	0.06				0.03	0.21	
217			412		120	25	0	25,000	0.18				0.17	1.55	
218			412		40	25	0	25,000	0.18				0.07	0.63	Vary ΔT, Ro
219			412		160	25	0	25,000	0.18				0.20	0.18	at Re=25,000
220			550		40	25	0	25,000	0.24				0.72	1.13	
221			550		120	25	0	25,000	0.24				0.30	2.73	
222			550		160	25	0	25,000	0.24				0.36	3.06	
223			825		40	25	0	25,000	0.36				0.28	2.39	
224			825		120	25	0	25,000	0.36				0.64	5.70	
225			825		80	25	45	25,000	0.34				0.42	3.66	
226			550		80	25	45	25,000	0.24				9.22	1.98	Angle
227			275		80	25	45	25,000	0.12				0.05	0.46	Variation
228			275		160	25	45	25,000	0.12				0.14	0.87	$\alpha = 45^0$
229			550		80	25	45	50,000	0.12				0.06	1.98	
230			550		160	25	45	50,000	0.12				0.14	3.49	

Streamwise location of test sections identified by A to R.
All four test section surfaces for streamwise locations A through R are heated.

- - - - - Leading test section surfaces

——— Trailing test section surfaces

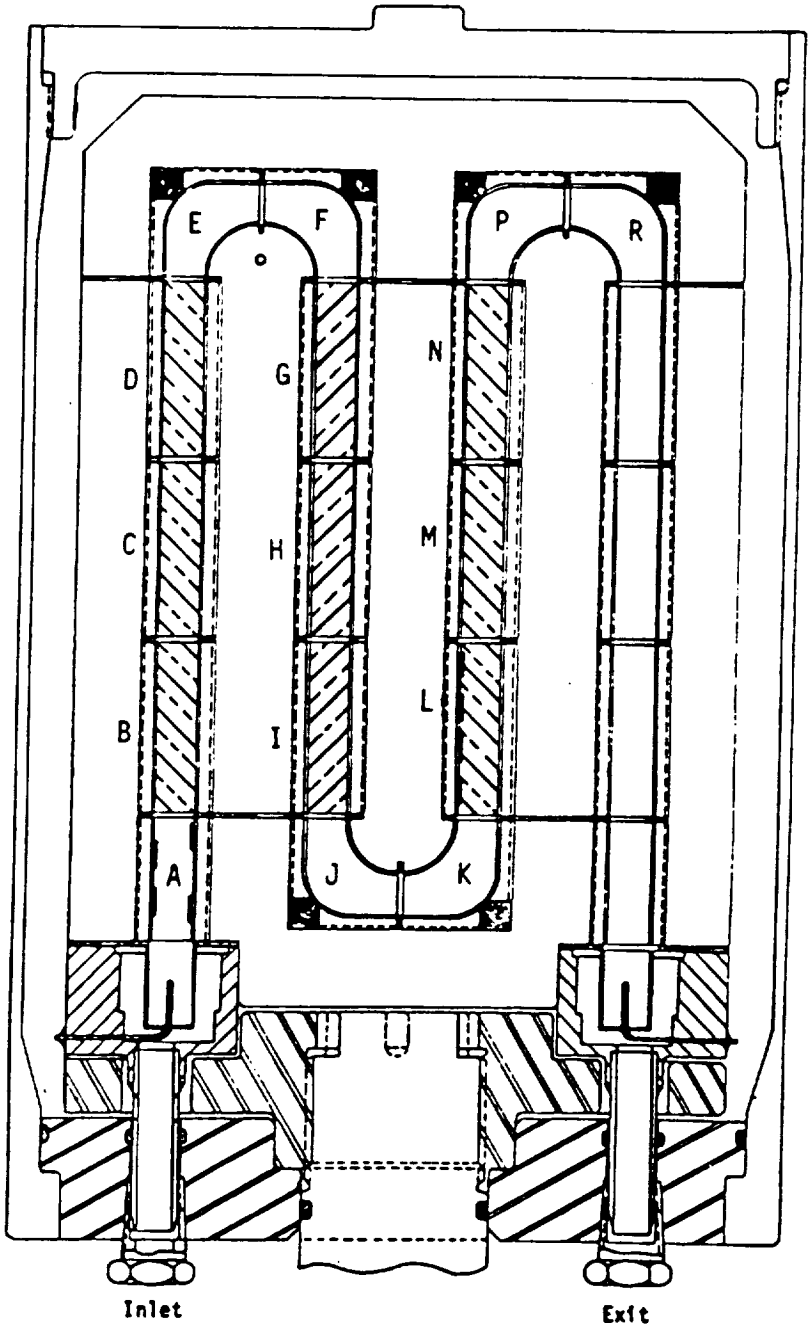

Figure 1 Cross Sectional View of Coolant Passage Heat Transfer Model Assembly With Skewed Trip Rough Walls

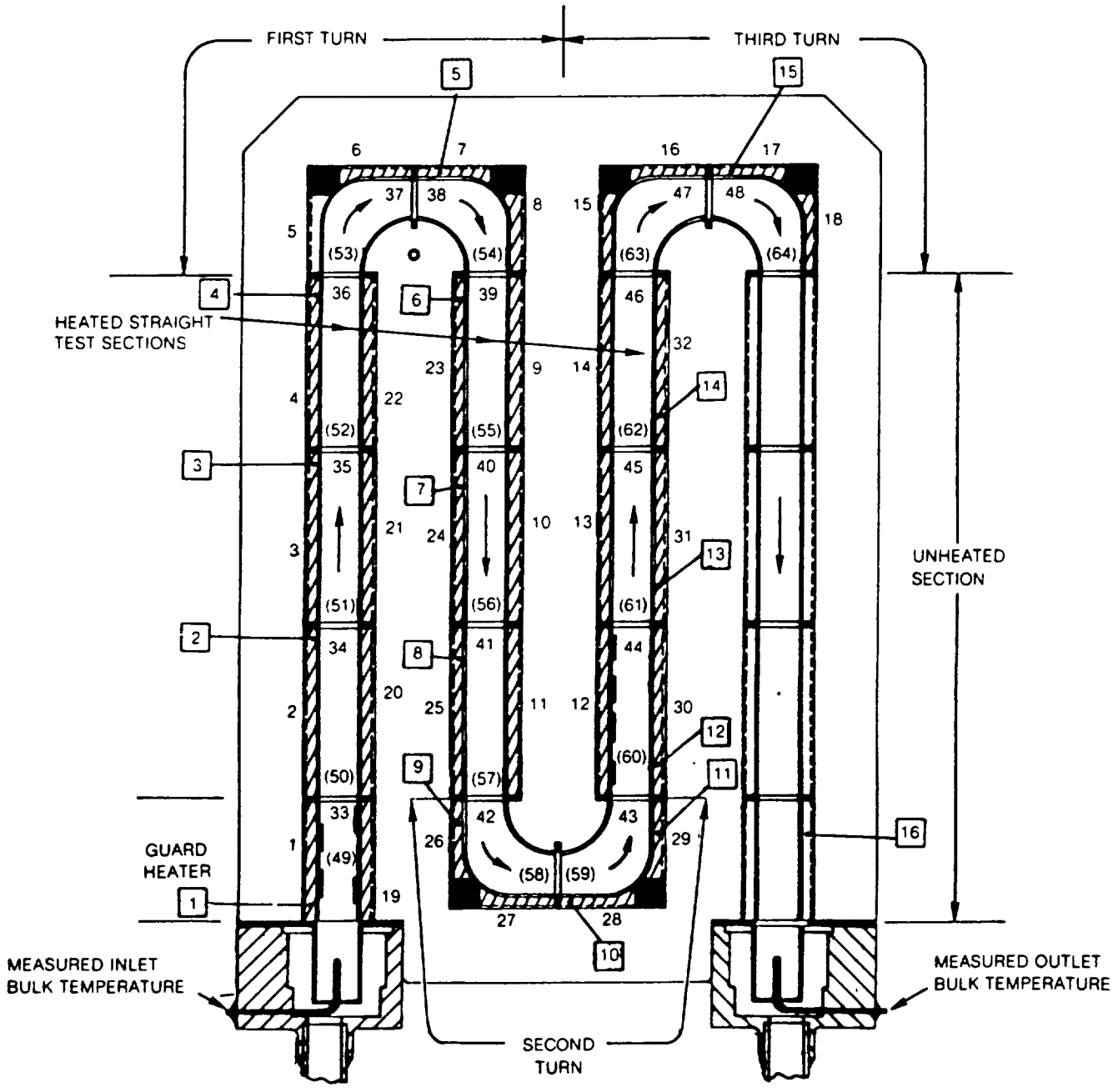

Figure 2 Instrumentation Plan for Coolant Passage Heat Transfer Model

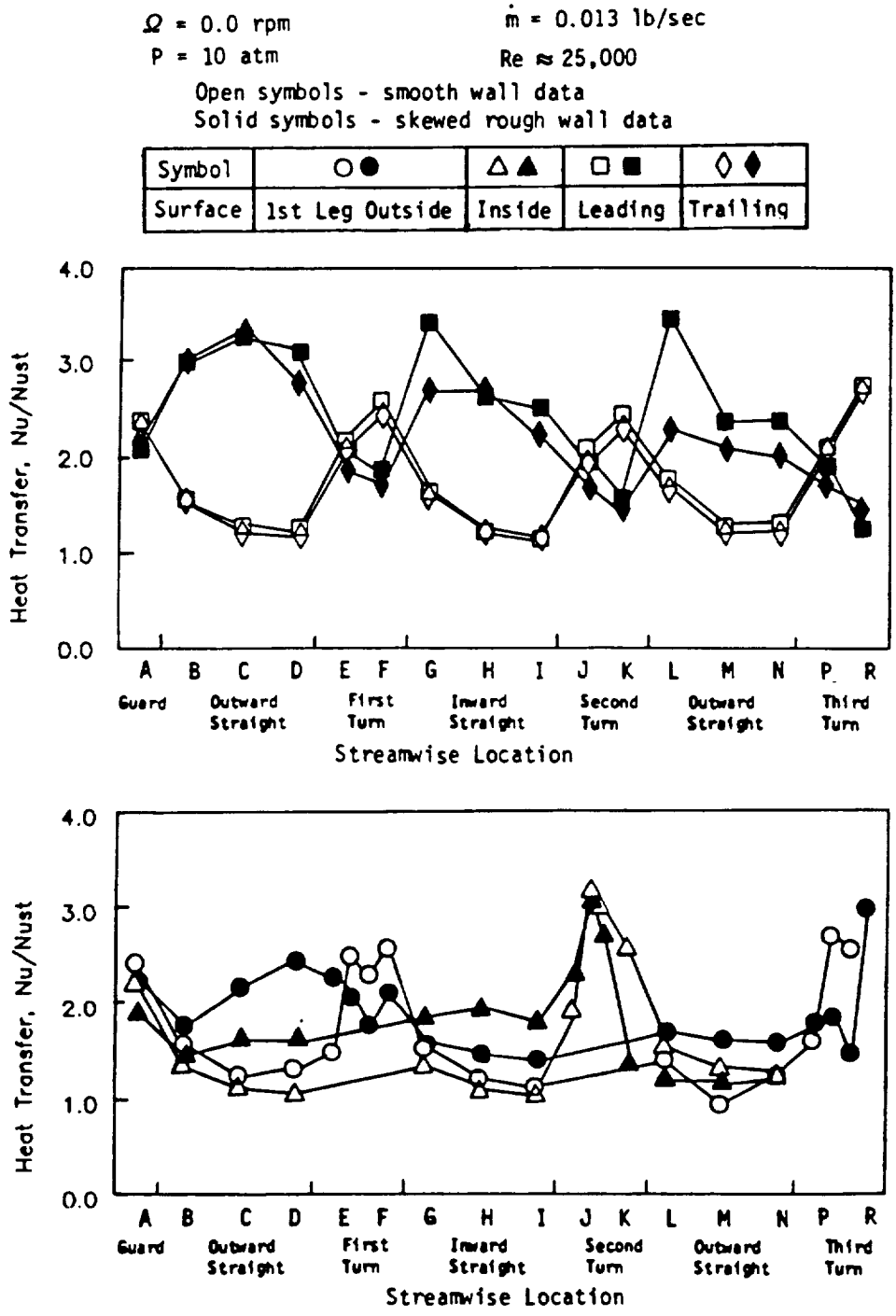

Figure 3 Comparison of Heat Transfer Results for Smooth Wall and Skewed Rough Wall at Baseline Stationary Flow Conditions

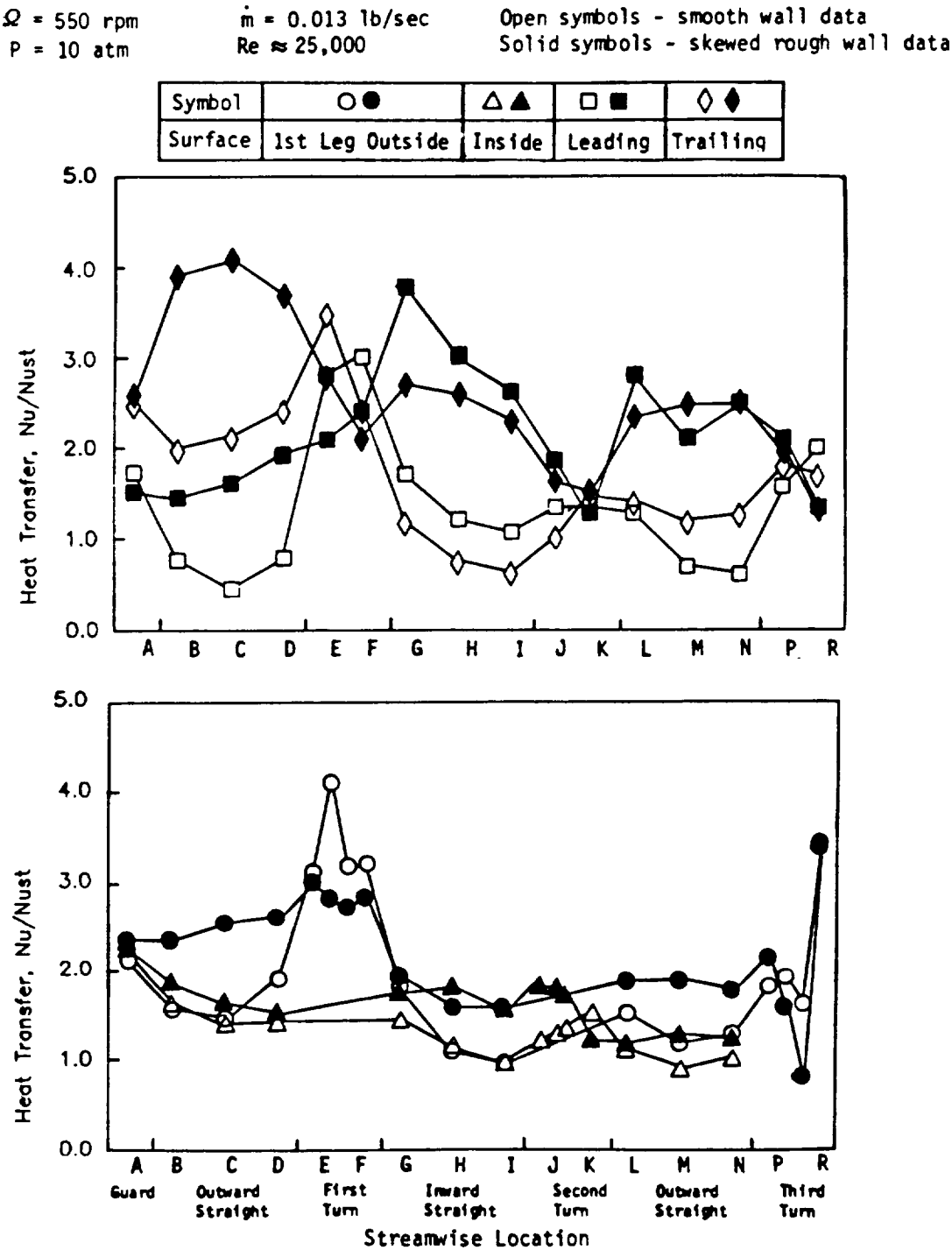

Figure 4 Comparison of Heat Transfer Results for Smooth Wall and Skewed Rough Wall at Baseline Rotating Flow Conditions

$\Delta T = 80^{0}$ F Re ≈ 25,000

Symbol	□	△	◇	×
Rotation Number	0	0.12	0.24	0.36
Speed (rpm)	0	275	550	825

a) Leading Surfaces 33-48

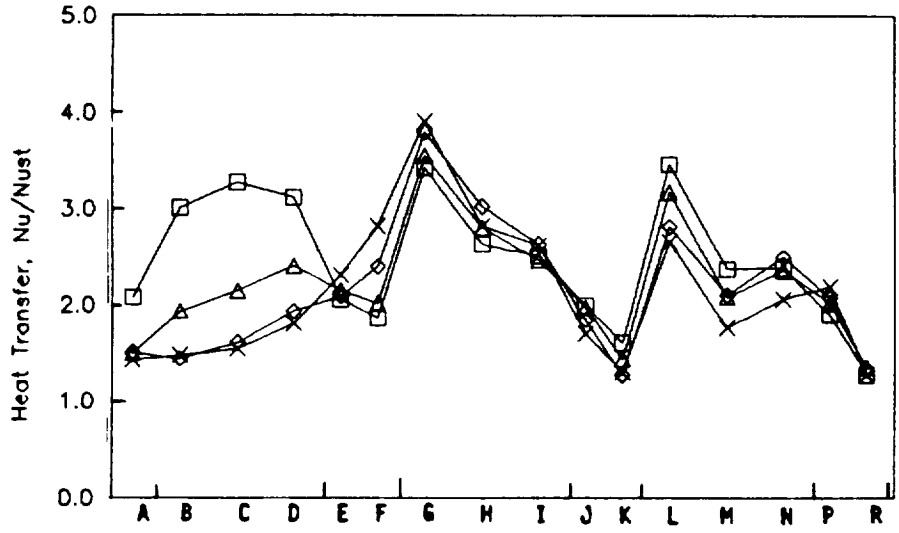

b) Trailing Surfaces 49-64

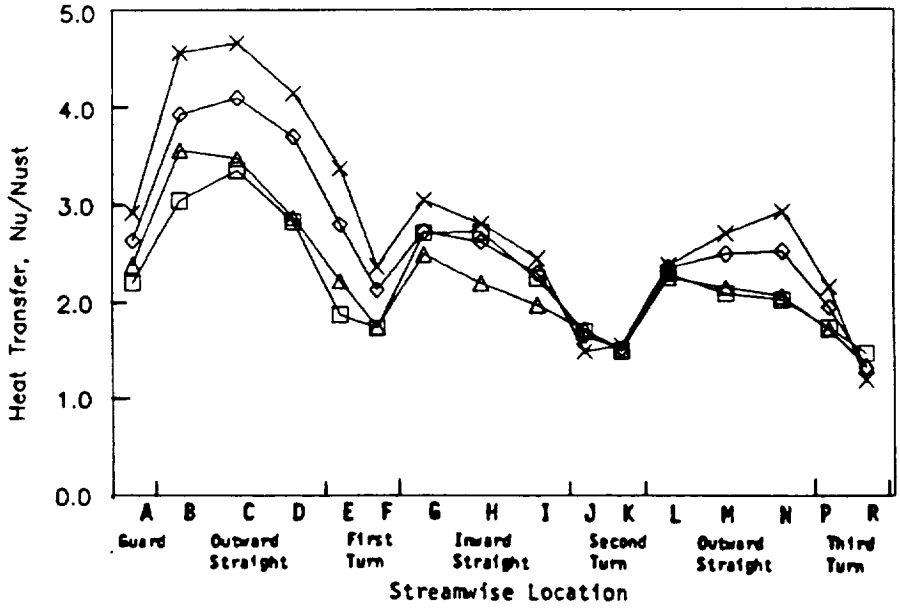

Figure 5 Effect of Rotation of Heat Transfer Results for Skewed Trip Rough Wall Model

$\Delta T = 80^0$ F Re ≈ 25,000

Symbol	□	△	◇	×
Rotation Number	0	0.12	0.24	0.36
Speed (rpm)	0	275	550	825

c) Side Wall Surfaces 1-18

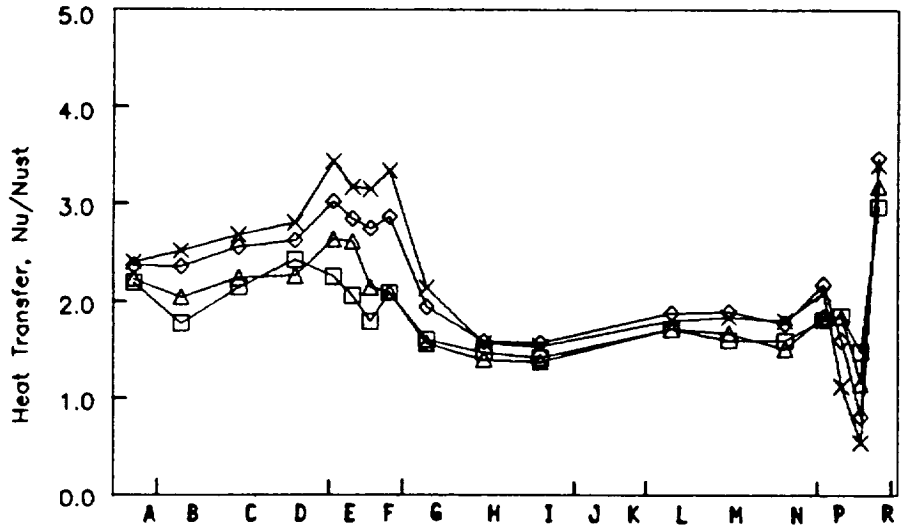

d) Side Wall Surfaces 19-32

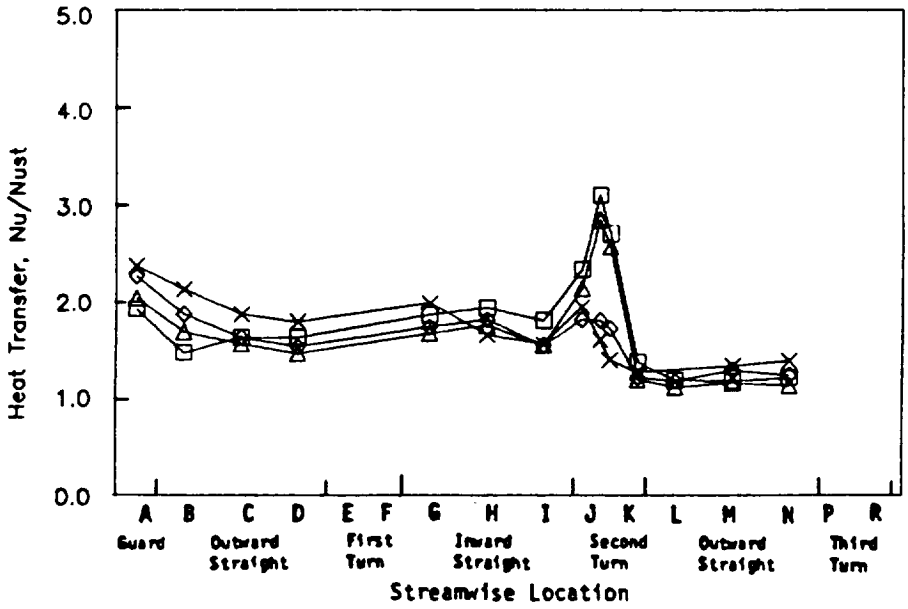

Figure 5 (Cont'd) Effect of Rotation of Heat Transfer Results for Skewed Trip Rough Wall Model

Ω = 550 rpm Re ≈ 25,000

Symbol	□	△	◇	×
$\Delta\rho/\rho$	0.06	0.11	0.15	0.19
Temp. Diff. (°F)	40	80	120	160

c) Side Wall Surfaces 1-18

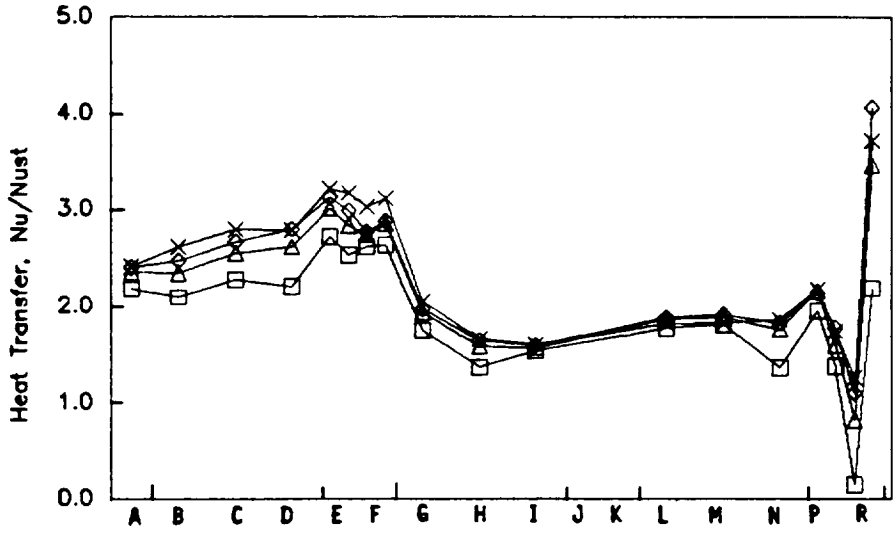

d) Side Wall Surfaces 19-32

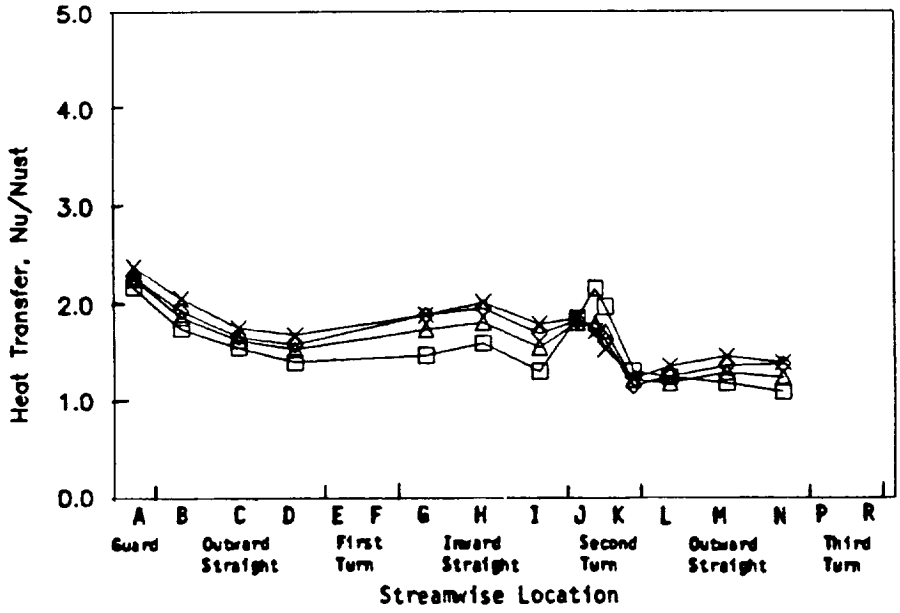

Figure 6 Effect of Density Ratio on Heat Transfer Results for Skewed Trip Rough Wall Model

Ω = 550 rpm Re $\approx$ 25,000

Symbol	□	△	◇	×
$\Delta\rho/\rho$	0.06	0.11	0.15	0.19
Temp. Diff. (°F)	40	80	120	160

a) Leading Surfaces 33-48

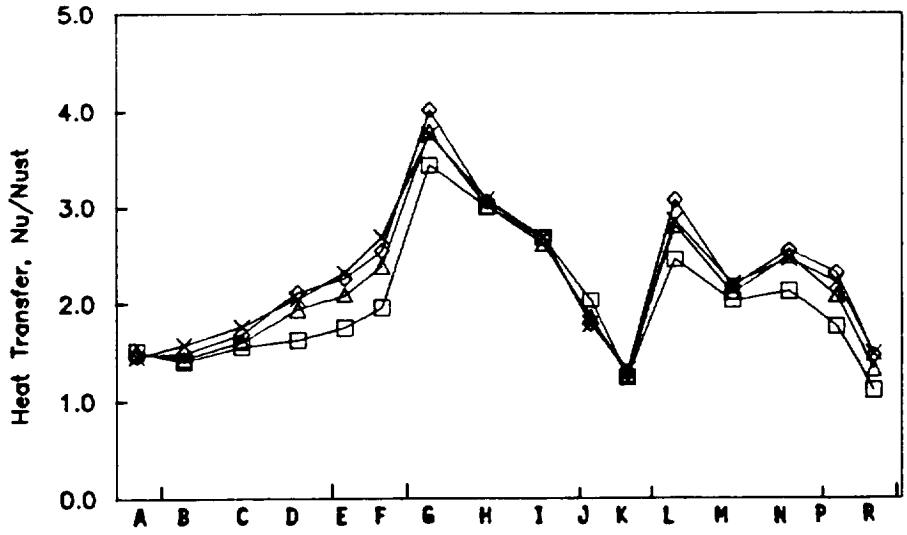

b) Trailing Surfaces 49-64

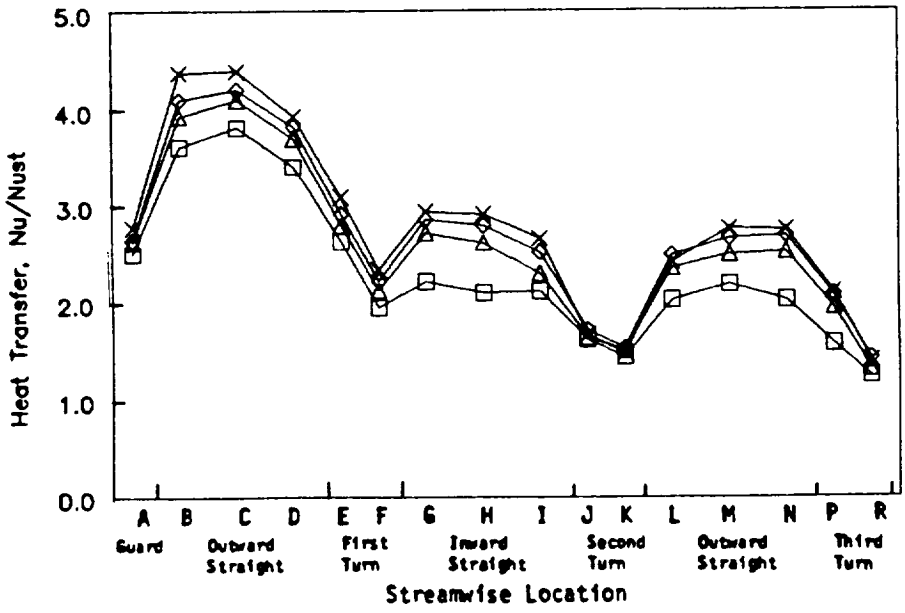

Figure 6 (Cont'd) Effect of Density Ratio on Heat Transfer Results for Skewed Trip Rough Wall Model

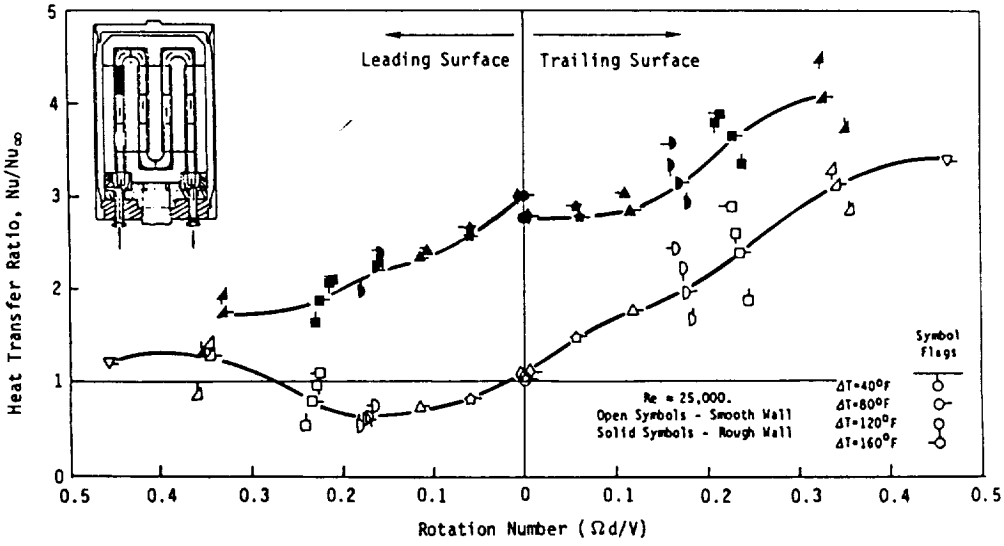

Figure 7 Effect of Rotation on Heat Transfer Ratio for Smooth Wall and Skewed Rough Wall Models

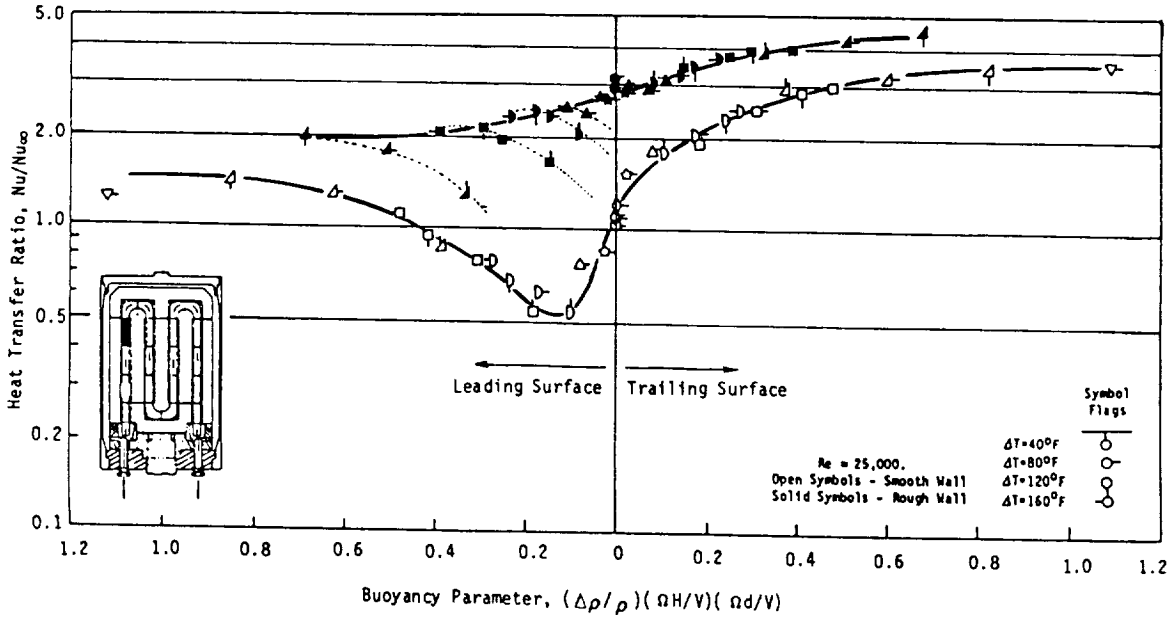

Figure 8 Effect of Buoyancy Parameter on Heat Transfer Ratio for Smooth Wall and Skewed Rough Wall Models